TEM vs STEM

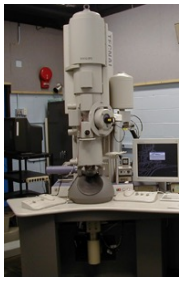

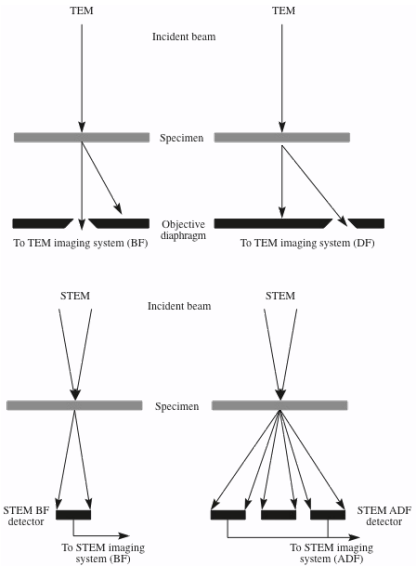

Why Bother??

1

TEM/STEM design

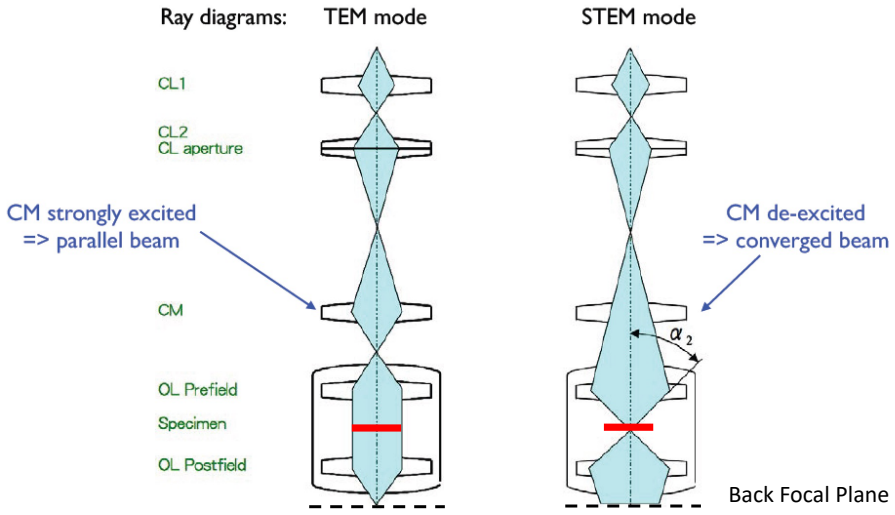

2

Zaluzec – 2023

Crewe FEG/STEM ANL 1965 -> Uof Chicago 1966

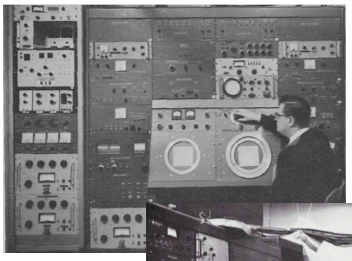

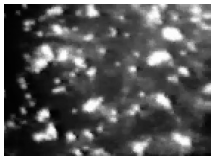

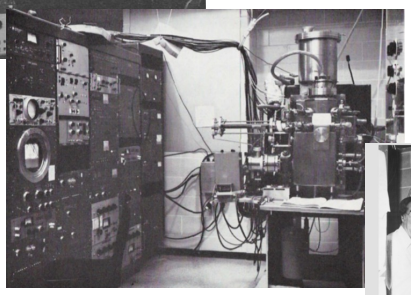

Albert Crewe, Mike Isaacson, Dave Kopf, Mark Utlaut, Mitsuo Ohtsuki

3

Zaluzec – 2023

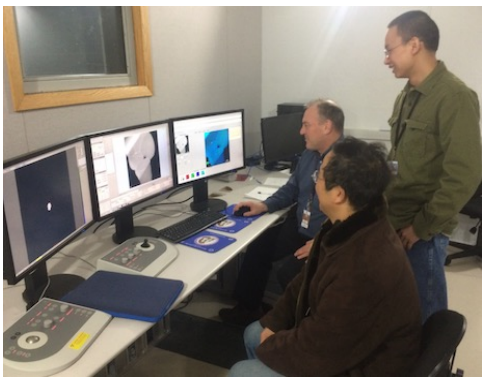

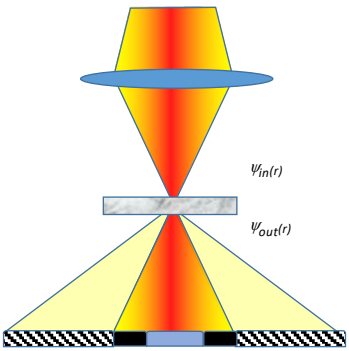

$I_D(k,r) = |\Psi_{out(r)}\ \Psi^*_{out\ (r)}|^2$

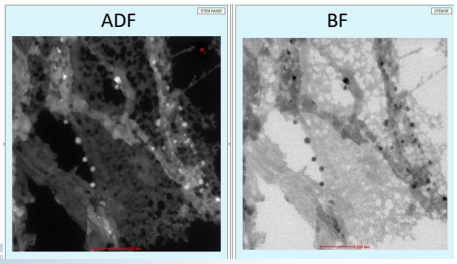

4

Reciprocity – STEM vs. CTEM

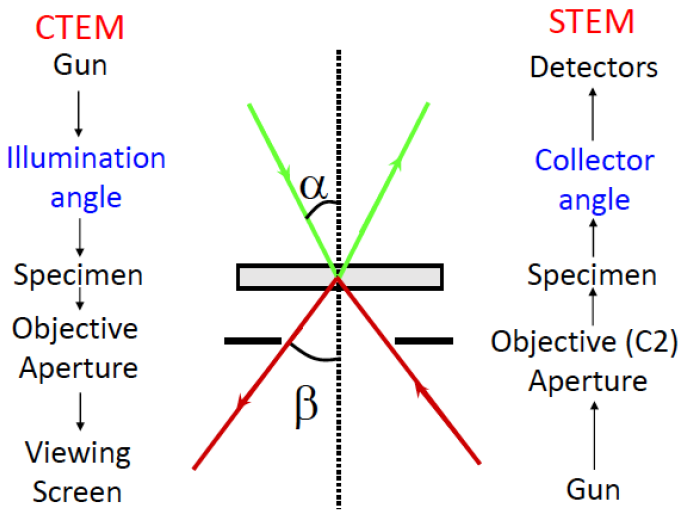

Based on slide by Prof D.A.Muller, Cornell (2004)

5

Zaluzec – 2023

Convergence and collection angles

- The focused probe is a convergent electron beam. The BF and DF detectors are radially symmetric. Therefore all of them are characterised by angles – angle of convergence for the beam; collection of scattering angles for the detectors
- The convergence semi-angle of the probe is called α
- A collection semi-angle for a detector is called β
- Knowledge of these angles is important for STEM imaging

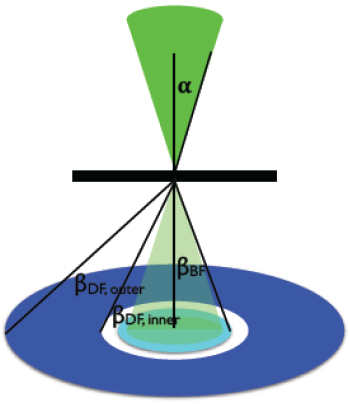

6

Zaluzec – 2023

STEM generally use Condensor Double Deflection Coils to Translate the beam across the specimen

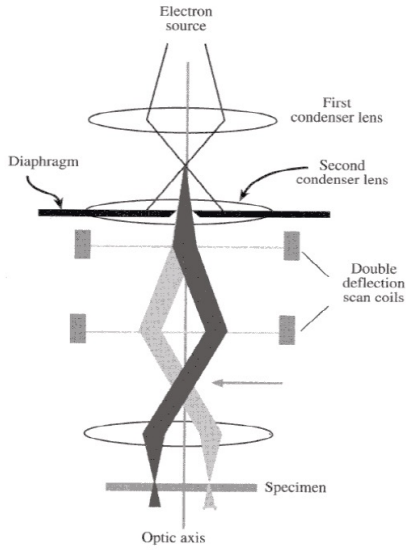

7

Zaluzec – 2023

Semi-conductor detector:

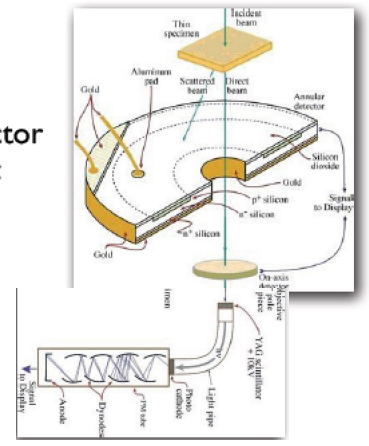

Scintillator photomultiplier (PMT) detector:

8

STEM Detectors
Can be a variety of shapes
and configurations.

Annular Detectors with "hole"
allow both Images
and EELS Data to
be acquired simultaneously

Today, the STEM detector is
a segmented array of detectors
Whose signals can be combined.

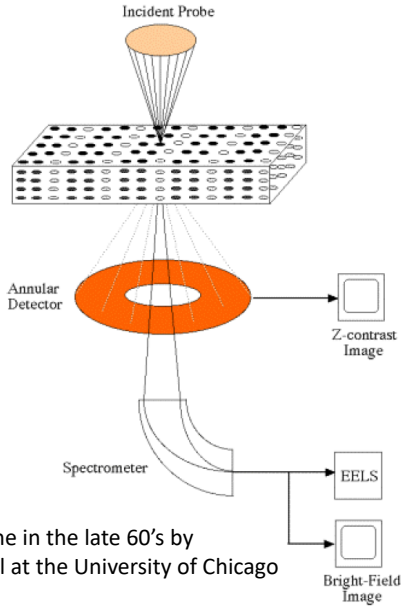

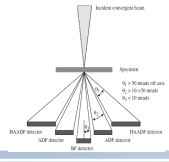

This was first done in the late 60's by
Albert Crewe etal at the University of Chicago

9

STEM Images

In a STEM the scattered electrons fall onto the ADF detector. This gives rise to a fundamental difference between the TEM and STEM DF modes:

- DF TEM images are usually formed by permitting only a fraction of scattered electrons to enter the objective aperture.
- STEM images are formed by collecting most of the scattered electrons on the ADF. Therefore, STEM ADF images are less noisy than TEM DF images.
- Because lenses aren't used to form the STEM image, the ADF images don't suffer aberrations (chromatic, spherical aberrations, for instance), as would the equivalent off-axis TEM DF image.
- STEM images generally only show better resolution than TEM images when thick specimens are being imaged. This is because the chromatic aberration effects from thicker specimens do not affect the STEM images.
- If contrast is more important than resolution, then a STEM is more useful. Indeed, in a STEM, you can study unstained polymer specimens which would show negligible contrast in a TEM.

10

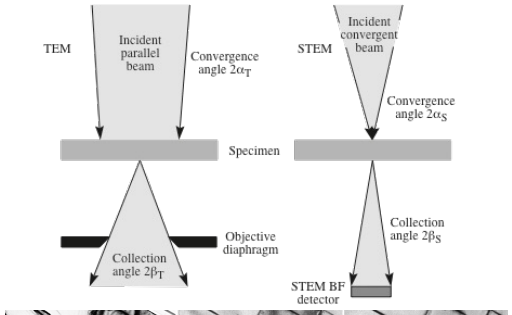

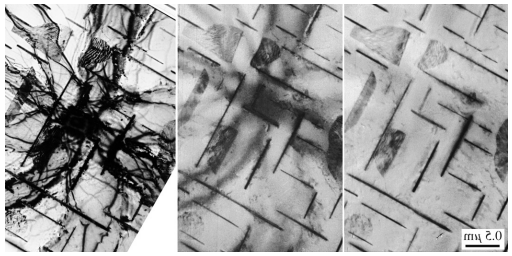

TEM | STEM with smaller β | Regular STEM

11

Imaging Mode & ROI Location: TEM vs STEM

(A) particle location

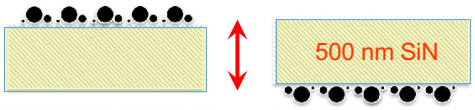

12

Rutherford scattering

- Coulombic interaction with the electron cloud → low angle scattering
- Coulombic interaction with the nucleus → higher-angle scattering
- Rutherford cross-section for high-angle scattering by nucleus alone:

$$\sigma_R(\theta) = \frac{e^4 Z^2}{16(4\pi\varepsilon_0 E_0)^2} \frac{d\Omega}{\sin^4 \frac{\theta}{2}}$$

- Including screening and relativistic correction:

$$\sigma_R(\theta) = \frac{Z^2 \lambda_R^4}{64\pi^4 a_0^2} \frac{d\Omega}{\left[\sin^2\left(\frac{\theta}{2}\right) + \frac{\theta_0^2}{4}\right]^2}$$

- When scattering angle > screening parameter θ_0 the electron nucleus interaction is dominant (E_0 is in keV); e.g. Cu, 200 keV beam $\theta_0 \approx 25$ mrad

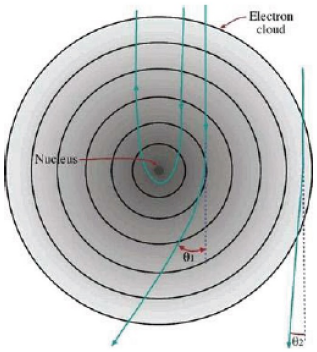

$$\theta_0 = \frac{0.117 Z^{1/3}}{E_0^{1/2}}$$

13

Z Contrast Image

- The method of Z-contrast imaging utilizes a post-specimen annular detector. This arrangement results in desirable effects in connection with the image contrast for crystalline specimens orientated close to their zone axes, or for small particles comprising elements of high atomic number. Many technologically interesting problems involve the interfaces and defects of such crystals and the knowledge of the size, spatial distribution and composition of such particles. Here, the Z-contrast image has important advantages over other image types. Intensities are easier to interpret in terms of the physical specimen structure and they are approximately proportional to the square of the atomic number (Z) of the elements present in each part of the specimen. Also, resolution approaches twice that of a bright-field phase-contrast image. The technique can be performed in parallel with other analytical experiments that yield complementary structural information.

Rutherford Scattering Cross-section

$$\sigma(\theta) = 1.62x10^{-14} \frac{Z^2}{E_0^2} \cot^2\left(\frac{\theta}{2}\right)$$

14

High Angle Annular Dark Field (HAADF) STEM

- An annular detector whose inner radius is > limit of the ZOLZ*
- The outer radius varies from 2-5 the inner radius – not critical
- Scattering is largely due to inelastic thermal diffuse (TDS) scattering
- Scattering here is very weak and a very efficient detector is required
- At such angles scattering the signal is **monotonic** and is **proportional to Z^n** where n is >1
- As such this technique of often called 'Z-contrast STEM'

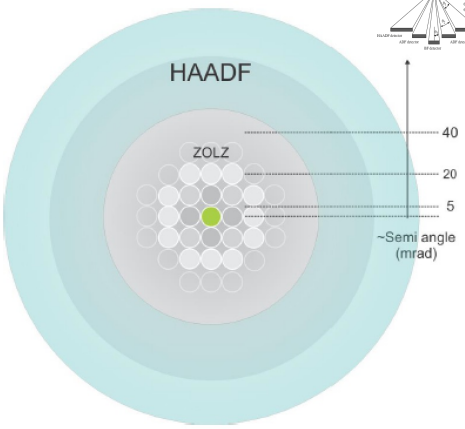

The blue detector shows a typical HAADF detector geometry where outer angle is ~2x the inner (JEOL, Gatan, FEI type)

*Howie A., *Journal of Microscopy* **117** 11-23 (1979)

15

Zaluzec – 2023

STEM Detectors & Contrast

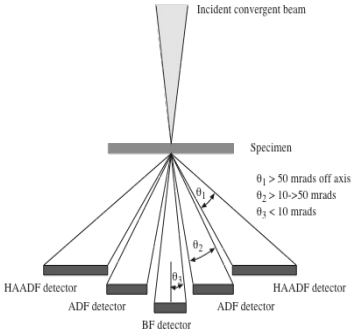

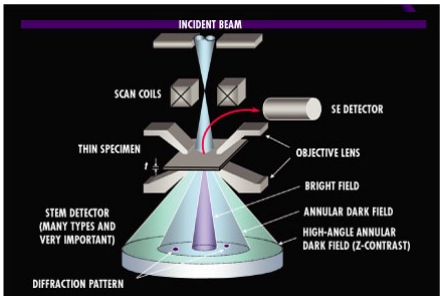

HAADF
Si/Ge
MultiLayer

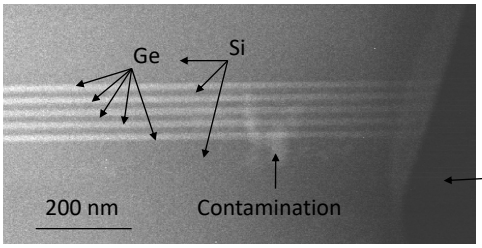

16

HAADF STEM
Pd-Sb-Mo on Titania

High Angle Annular Dark Field STEM Images

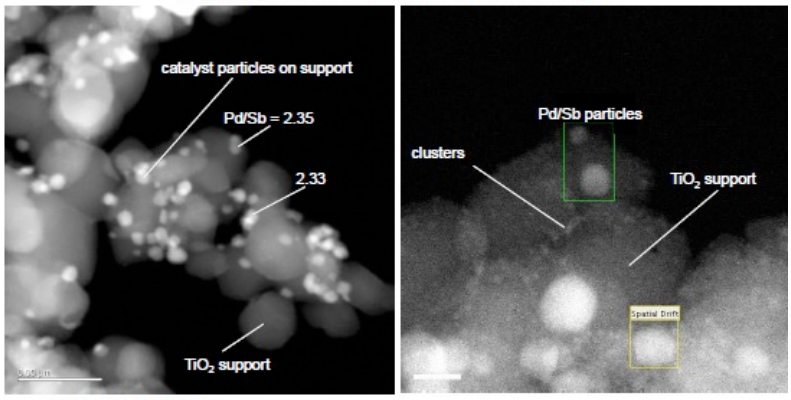

17

STEM HAADF Imaging of $(BaTiO_3)_4/(CaTiO_3)_4$ Ferroelectric Superlattice along [110]

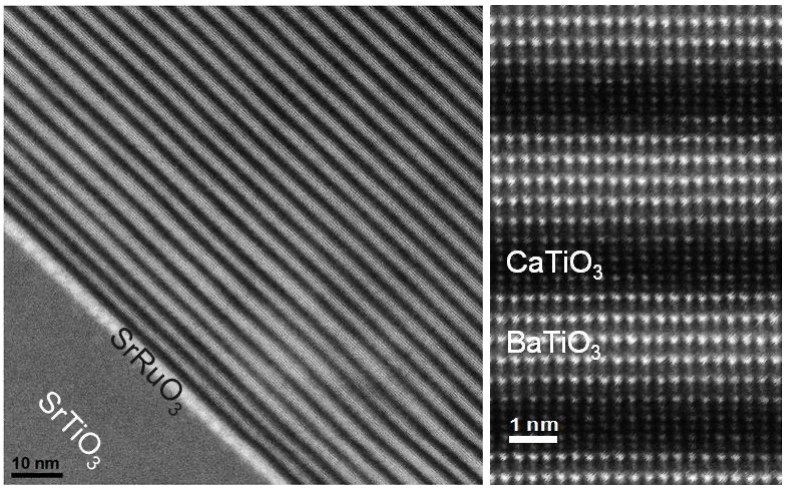

HAADF shows high quality of the superlattice film with good Z contrast among Ba, Ca, and Ti columns. Oxygen columns are not observed. No superstructure is observed.

18

Zaluzec – 2023

Single Atom Imaging
Pt on UltraNanoCrystalline Diamond (UNCD)

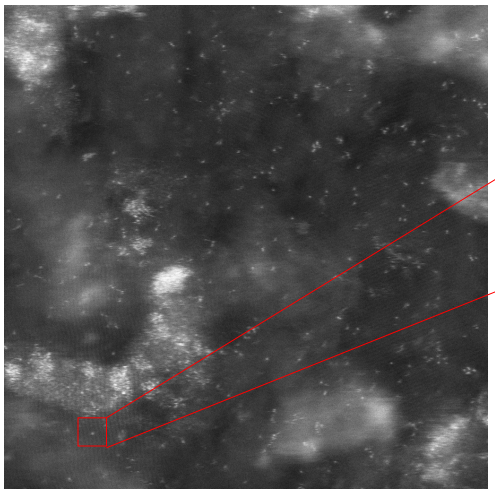

300 kV
Analytical Pico Probe
Prototype Testing

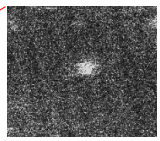

UNC Diamond Lattice
Visible in Background

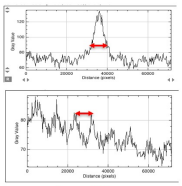

d_{111} = 206 pm

19

Zaluzec – 2023

HAADF/Z-contrast imaging

Z-contrast examples:

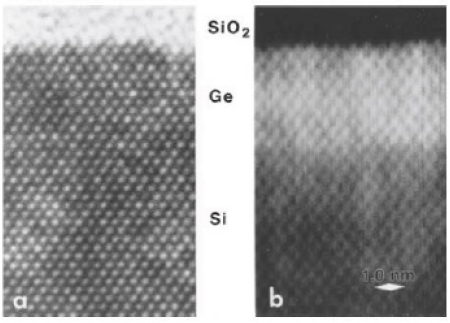

Figure 1–16. Images of a Ge film grown epitaxially on Si by an implantation and oxidation method. (**a**) Conventional TEM image from a JEOL 200CX, (**b**) Z-contrast image obtained with a VG Microscopes HB501UX clearly delineating the Ge layer, reproduced from Pennycook (1989a).

HREM - TEM HAADF STEM

20

Coherent vs Incoherent imaging

- In the 1970s, biologists Engel et al. and Misell et al. proved that the integration of signals on an ADF detector represents a convolution of intensities instead of amplitudes:

$$I(\mathbf{R}_0) = \int |\varphi(\mathbf{R})|^2 |P(\mathbf{R} - \mathbf{R}_0)|^2 d\mathbf{R},$$

- The fundamental equation for incoherent images is therefore obtained:

$$I(\mathbf{R}_0) = |\varphi(\mathbf{R}_0)|^2 \otimes |P(\mathbf{R}_0)|^2$$

- Compared to coherent – i.e. phase contrast – imaging, incoherent imaging has some specific (useful!) characteristics:
  - No image contrast inversion with defocus
  - "Camera-like characteristics"
  - Broad optical transfer function

21

Optical transfer function of incoherent imaging

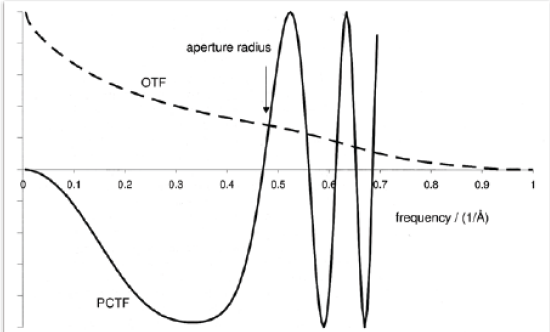

Figure 2-12. A comparison of the incoherent object transfer function (OTF) and the coherent phase-contrast transfer function (PCTF) for identical imaging conditions (V = 300 kV, C_s = 1 mm, z = −40 nm).

- Incoherent imaging gives a better spatial resolution than coherent imaging
- This was proved by Lord Rayleigh in 1896 (Phil. Mag. **42**, p. 167); the Rayleigh criterion for resolution basically applies

"Scanning Transmission Electron Microscopy", P.D. Nellist, in *Science of Microscopy Vol. 1*, Springer 2007

22

High Angle Annular Dark Field (HAADF) STEM

- HAADF STEM is directly interpretable – it is an incoherent image (unlike phase contrast) – a bright dot appears at an atom column. No matter the defocus.
- There cannot be a contrast reversal in an HAADF STEM image – as long as the sample is not VERY thick or VERY high atomic number.
- It is also proportional to thickness making it ideal for **tomography**
- It is very insensitive to diffraction alignment – just place the pattern inside the hole and you will get an image

As such HAADF STEM is very popular as it is extremely **robust** and **simple..**

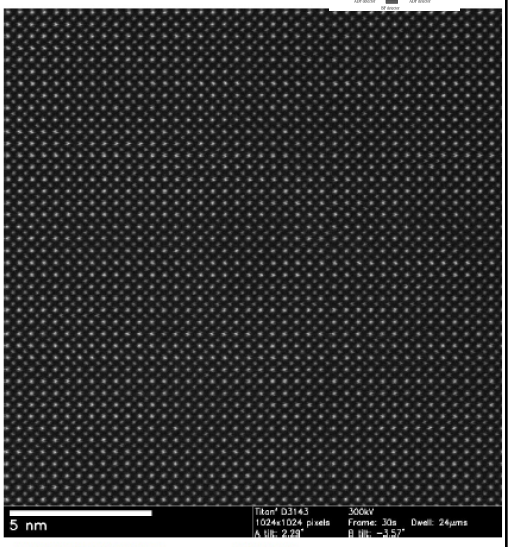

HAADF STEM image of $SrTiO_3$ M. Weyland 2018

23

HAADF STEM Z-contrast – actually not so simple..

- HAADF stem is **proportional** to thickness…
- HAADF stem is **proportional** to the atomic number…
- BUT also to the **crystal orientation**!
- As the crystal tilts the beam orientation relative to the crystal changes..
- Therefore the total amount of channelling and scattering changes…
- HAADF STEM is **robust** BUT **qualitative** without knowing the exact crystal structure, it's exact orientation and thickness it cannot be quantitative

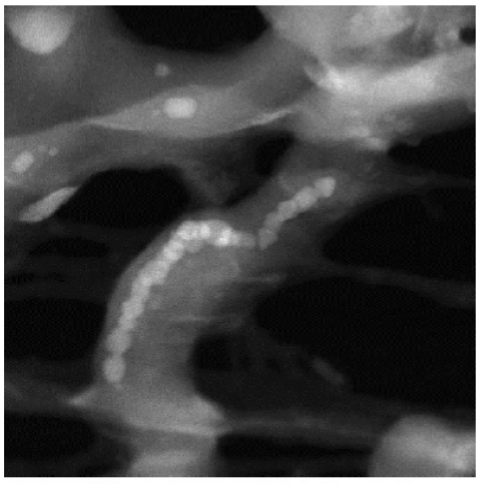

HAADF STEM tilt series (FEI F20 @ 200kV) of a Magnetotactic bacteria (strain MV-1), containing chains of magnetosomes – Single crystal Fe_2O_3 nanomagnets.

M. Weyland 2018

24

Centred Bright Field (BF) STEM – phase contrast in convergent beam

- By reciprocity any illumination condition in TEM can be achieved by modifying the collection angle in STEM
- A phase contrast STEM image can be formed that is equivalent to its TEM counterpart
- However an infinitely small detector (approximates a parallel beam!) is not efficient*
- A small (<5 mrad) detector is a reasonable compromise

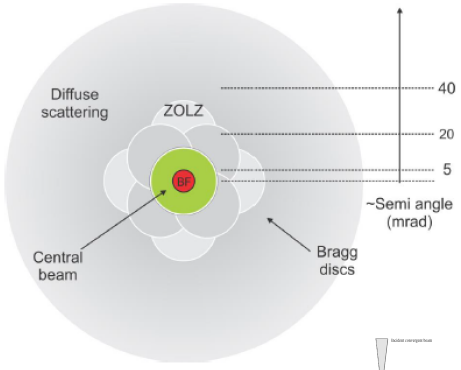

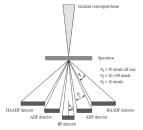

* In a parallel beam TEM ALL the electrons will contribute to the phase contrast image – in a convergent bema STEM only a small fraction will (and we typically have lower current already to get a small probe)

M. Weyland 2018

25

Centred Bright Field (c-BF) STEM – phase contrast in convergent beam

- Centred bright field STEM (c-BF) is the STEM analogue to phase contrast BF TEM without an Objective aperture
- It is **not robust** or **simple** – but can offer complementary information to HAADF especially when acquired simultaneously
- It is **very** sensitive to **defocus**
- It is **extremely** sensitive to crystal misalignment, poorly centred detector and astigmatism. All must be perfect.

As such BF STEM is not very popular as it is difficult to use.. BUT when paired with HAADF STEM it can be very useful

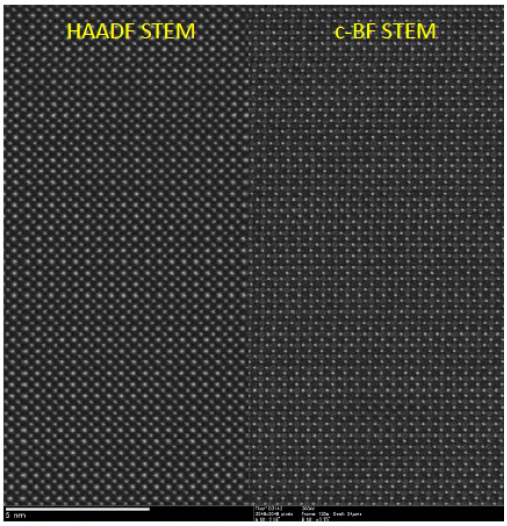

Simultaneous HAADF and c-BF STEM image of STO – note bright O columns in c-BF image

M. Weyland 2018

26

Incoherent bright field (IBF)*

- By opening up the bright field detector (or in practice reducing the camera length) we reach a point where we collect the entire ZOLZ (or more)
- This condition is called incoherent bright field (IBF) as it forms an incoherent STEM image (a practical inverse of HAADF)
- This is especially good for THICK and HIGH Z specimens – geometry means there can never be a contrast reversal
- Still lower contrast than HAADF in normal conditions

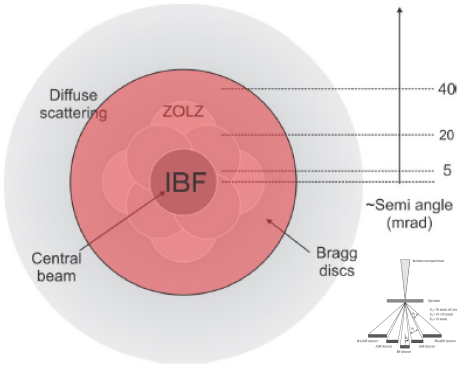

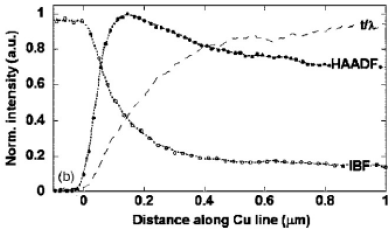

Plot of HAADF and IBF signals from a specimen of Cu of increasing thickness* note contrast reversal in HAADF

M. Weyland 2018

*Ercius et al, APL 88, p1 (2006)

27

Annular bright field (ABF)*

- Uses an annular detector placed on the central beam – spanning α/2 to α
- Creates a interpretable image that is 'absorption like' image across a wide range of **thickness** and **defocus**

- especially compared to BF

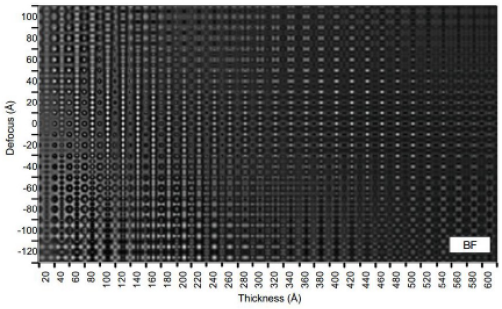

Simulation of c-BF STEM image for 110 STO from a range of thicknesses and defoci – note the rapid change in contrast *

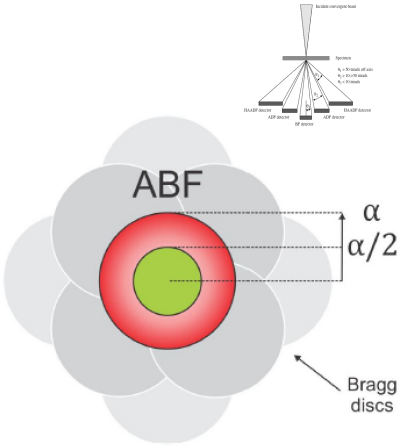

*Findlay et al, APL 95, 191913 (2009)
Findlay et al, Ultramicroscopy 110, p903 (2010)

M. Weyland 2018

28

Annular Bright Field (ABF) STEM – low Z columns

- Annular bright field STEM (ABF) produces a complementary image to HAADF STEM, with a very similar contrast profile and the *same optimal defocus*
- As long as it is set up carefully it is **robust** and **simple** to interpret – and can offer complementary information to HAADF especially when acquired simultaneously
- It is **extremely** sensitive to crystal misalignment, poorly centred detector and astigmatism. All must be perfect.

ABF is not a panacea – and needs care to use, especially on defective materials

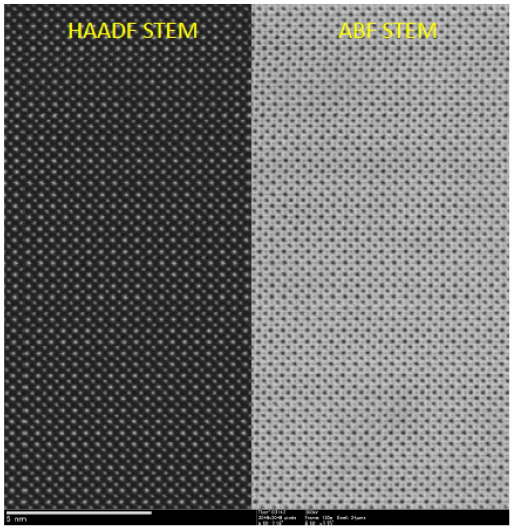

Simultaneous HAADF and ABF STEM image of STO – note Sr, Ti and O columns resolved

M. Weyland 2018

29

Low angle annular dark field (LAADF)

- Placing an annular detector with an inner angle slightly > α , collecting any Bragg scattering outside the central beam
- As such this mode is **very** sensitive to small changes in **lattice parameter** and **crystal orientation**
- It also retains Z-contrast
- Good for detecting small changes in structure – such as induced by strain or by small secondary phases
- Excellent for imaging dislocations

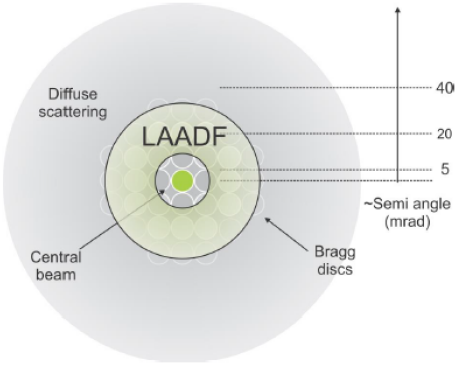

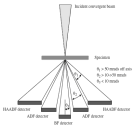

M. Weyland 2018

30

Differential Phase Contrast

- DPC requires a SEGMENTED detector of at least 2 sections – conventionally overlapping with the central beam
- Each segment is read out separately (so at least 2 and up to 16 channels)
- Like LAADF it is extremely sensitive to small changes in the first moment of the diffraction pattern
- The information from the segments can be used to provide a range of processed signals based on physical principles
- Not a new technique! (see Rose, 1974 and Dekkers 1974)

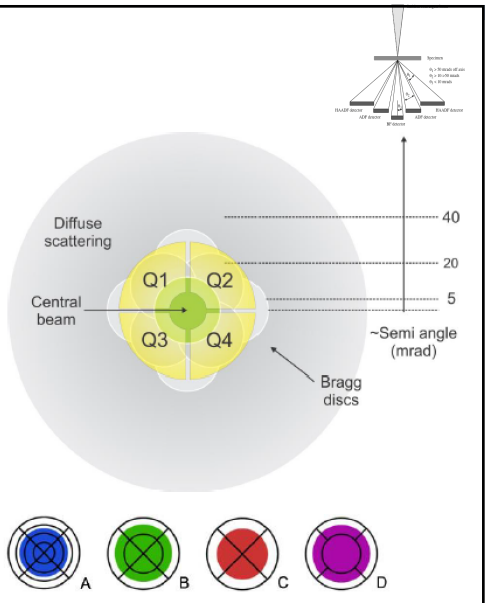

Above – a 4 quadrant DPC detector. Other designs (A-D) use up to 16 segments.. At least 2 are now commercial*

H Rose, Optik 39, p416 (1974) & N. H. Dekkers et al, Optik 41, p452 (1974)
*D Taplin, N. Shibata, M. Weyland and S.D Findlay, Ultramicroscopy 169, p69 (2016)

M. Weyland 2018

31

Position Resolved Diffraction (4DSTEM = Misnomer)

Replace the segmented Si Detector by a High Resolution ARRAY of sensors

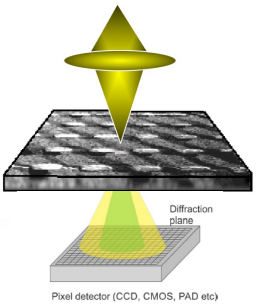

2001

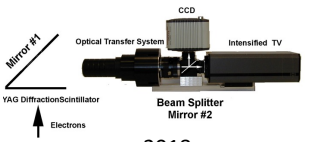

2018

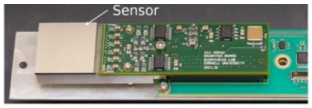

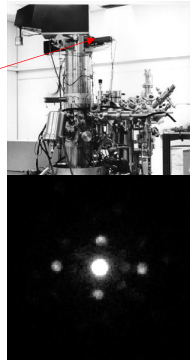

XY \ αβ	256^2	512^2	1024^2
64^2	262M	1G	4.2G
128^2	1G	4.2G	16.7G
256^2	4.2G	16.7G	67G
512^2	16.7G	67G	275G
1024^2	67G	275G	1T

t \ XY	128^2	256^2	512^2	1024^2
1µs	16 ms	65 ms	0.26 s	1.05 s
1ms	16 s	65 s	4.4 min	17.5 min
1 s	~4.5 hrs	~18 hrs	~3 days	~12 days
1 min	~11 days	~1.5 mnths	~ 6 mnths	~2 yrs

Comparisons of Dynamic Range Detectors

Cornell EMPad 128x128 – 30 bit – 1.07x 10^9cnts
PN Sensor - 256x256 – 16 bit - 6.5 x 10^4cnts
K2/OneView DE Array - 2Kx2K – 16 bit - 6.5 x 10^4cnts
Merlin – Quantum Detectors - ?
LBNL DE Array - ?? TBD
Others…

32

Position Resolved Diffraction

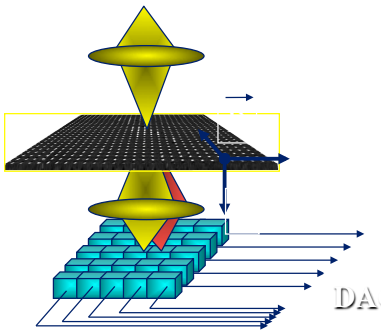

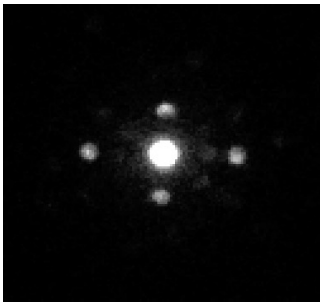

DAQ System

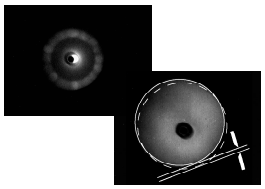

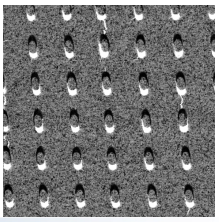

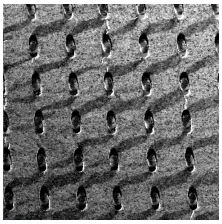

33

What Limits the ability to form a small probe?

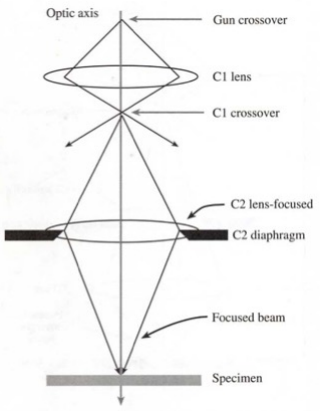

Aberrations

- Spherical
- Chromatic

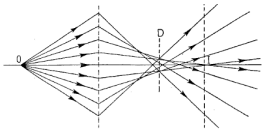

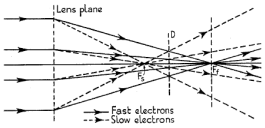

$$r_{sph} = C_s \beta^3$$

$$r_{chr} = C_c \frac{\Delta E}{E} \beta$$

Lens Aberrations

34

The optimal probe size?

Choosing the objective aperture hence the convergence angle (α) is a balance

We can add the various factors in quadtrature to estimate the optimal α

$$d = \sqrt{d_g^2 + d_d^2 + d_s^2 + d_c^2 + d_i^2 + \cdots}$$

C_s and the diffraction limit are the largest Contributors, but there are others;

d_c - Chromatic aberration C_c
(will become important at low kV)

d_i – Incoherent aberrations C_c
(this term sums together all the instabilities in the Environment into one term – more on this later)

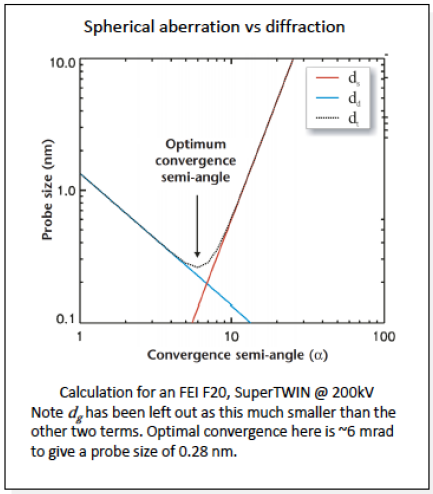

Calculation for an FEI F20, SuperTWIN @ 200kV
Note d_g has been left out as this much smaller than the other two terms. Optimal convergence here is ~6 mrad to give a probe size of 0.28 nm.

M. Weyland 2018

35

Optimising the STEM probe size – wave optical model

The classical approach is intuitive BUT neglects wave optics, overestimates the source contribution, – and results in a significant **overestimation** of probe size.

A more complete wave-optical model, based on the Scherzer aberration function, can be formulated*. This allows compensating for C_s by a small defocus, and leads to estimates for;

Minimum probe size *(d_0)*

$$d_0 = 0.43 C_s^{1/4} \lambda^{3/4}$$

Optimal convergence semi-angle *(α_0)*

$$\alpha_0 = \left(\frac{4\lambda}{C_s}\right)^{1/4}$$

For the previous example of the F20 the new d_0 is 0.16 nm at an α of 9.6 mrad

* M.Weyland & D.A.Muller, FEI Nanosolutions 01, p 24 (2005)

36

Does α really matter?

- For getting the best out of your STEM this is CRITICAL
- Too small an aperture will leave you with a smaller probe (lower resolution)
- Worse, too large an aperture will introduce large probe tails, and reduce the intensity in the probe
- This will reduce contrast of high resolution features and create spurious long range intensity

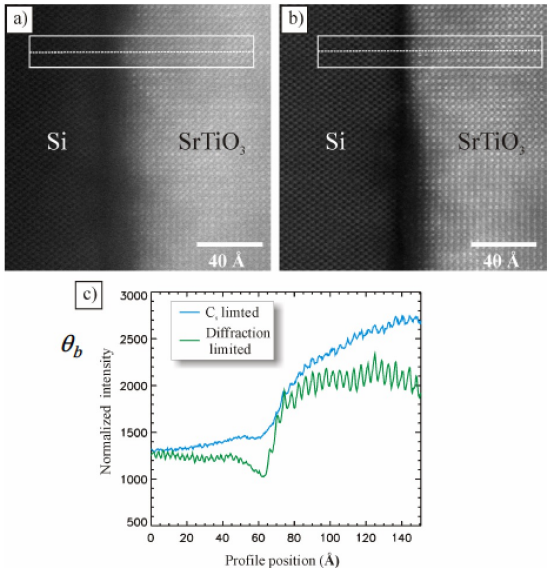

Effect of aperture radius/convergence angles on apparent interface width between Si and SrTiO3. a), b) STEM HAADF images acquired from the same area with a) Cs and b) diffraction limited optimal convergence semi-angle respectively. c) Line traces (averaged and normalized) through the interface, at the positions marked, for the two conditions.*

* M.Weyland & D.A.Muller, FEI Nanosolutions 01, p 24 (2005)

37

Zaluzec – 2023

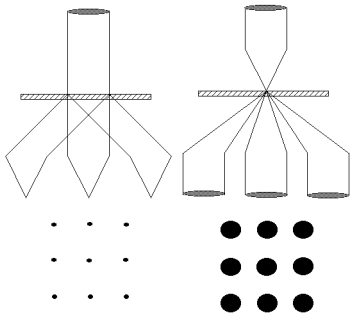

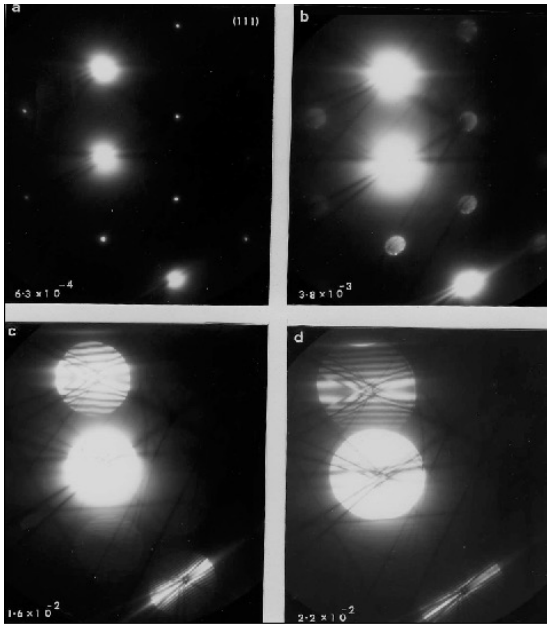

Notice, loss of definition of weak reflections !

38

Ronchigrams

- Rochigrams are point projection 'shadow' images of the electron probe interacting with the specimen formed at or near focus
- On an amorphous specimen they allow the determination and alignment of optical parameters including;

  Focus
  Astigmatism (2-fold)
  Beam Tilt (Rotation centre)
  C2 Aperture position

  Axial Coma (Cs corrected)

- On a crystal they allow accurate alignment of orientation AND focus

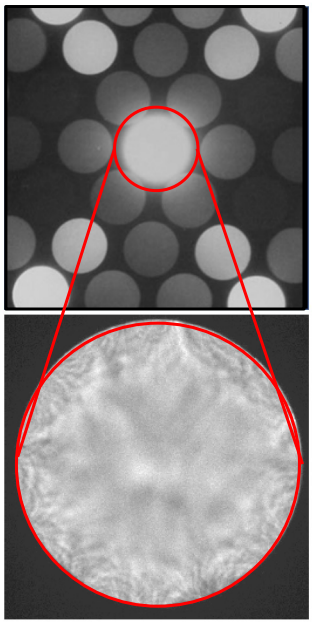

Aligned Rochigrams for Convectional (top) and C_s Corrected STEM systems (to scale) on an amorphous film

J. M. Cowley, *Ultramicroscopy* **4**, 413-418.(1979)
E. M. James, N. D. Browning, Ultramicroscopy, 78 (1999) 125-139

Based on slides by Prof D.A.Muller, Cornell (2004)

39

Zaluzec – 2023

Basics of shadow image formation

Assuming perfect optics

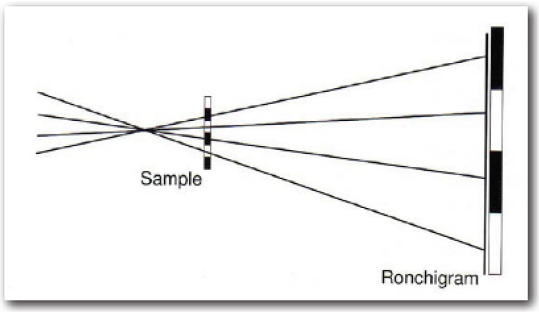

At overfocus the STEM detector plane is a shadow image of the sample
Magnification $M = d_{\text{probe-detector}}/d_{\text{probe-sample}}$

At underfocus the image will be magnified, but also *inverted*

Ronchigram is similar to defocused TEM diffraction pattern, blending image information with scattering angles

Diagram from: "Scanning Transmission Electron Microscopy", P.D. Nellist, in *Science of Microscopy Vol. 1*, Springer 2007

40

Ronchigram – Interpreting

For Cs>0, rays far from the axis are bent too strongly and come to a crossover before the gaussian image plane.

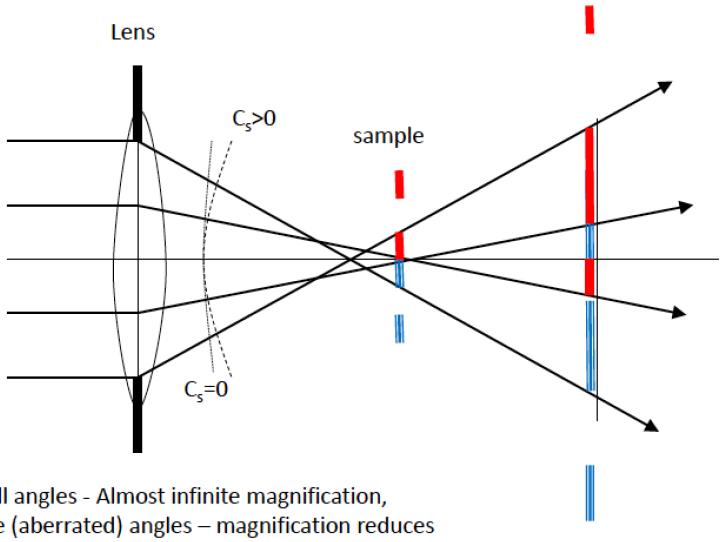

At small angles - Almost infinite magnification,
At large (aberrated) angles – magnification reduces

Based on slide by Prof D.A.Muller, Cornell (2004)

41

Ronchigram – Correction of severe astigmatism (Conventional)

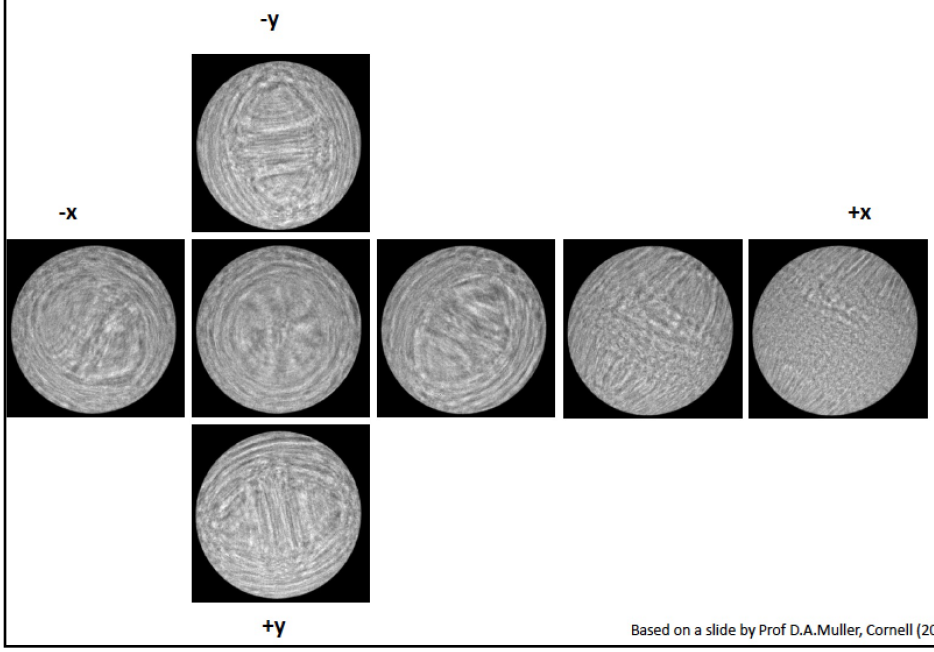

Based on a slide by Prof D.A.Muller, Cornell (2004)

42

Ronchigram – Though Focus (and aperture position)

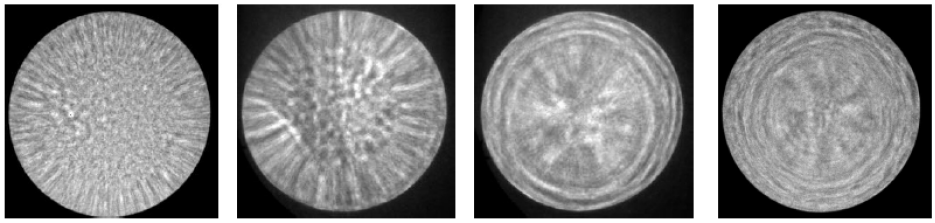

Underfocused → Focused

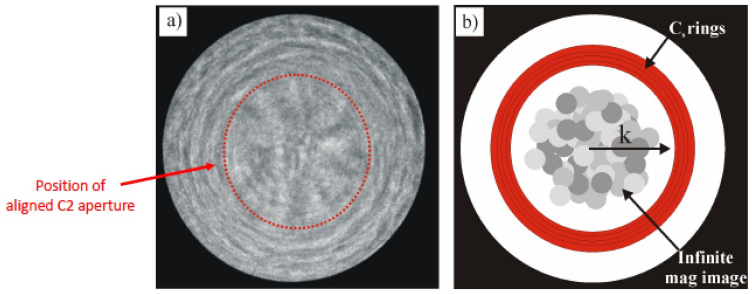

Based on a slide by Prof D.A.Muller, Cornell (2004)

43

Zaluzec – 2023

Focusing with the Ronchigram

- In practice:
  - Reduce under-focus until infinite-magnification rings are of minimum diameter => optimum defocus (c.f. Scherzer defocus in HR-TEM)

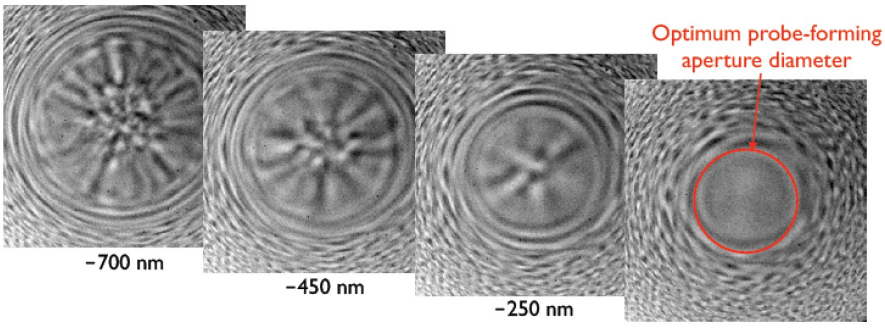

  - Fit probe-forming aperture to the "sweet spot" region of constant phase within this diameter

44

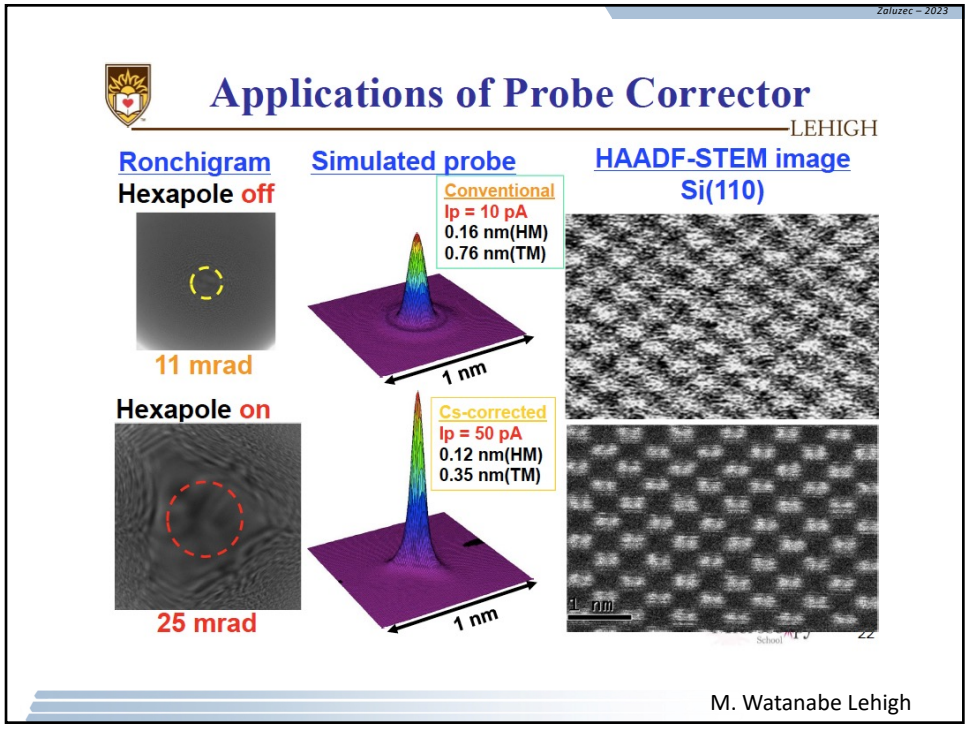
Zaluzec – 2023
Applications of Probe Corrector
LEHIGH
Ronchigram
Hexapole off
11 mrad
Hexapole on
25 mrad
Simulated probe
Conventional
Ip = 10 pA
0.16 nm(HM)
0.76 nm(TM)
1 nm
Cs-corrected
Ip = 50 pA
0.12 nm(HM)
0.35 nm(TM)
1 nm
HAADF-STEM image
Si(110)
1 nm
M. Watanabe Lehigh

45

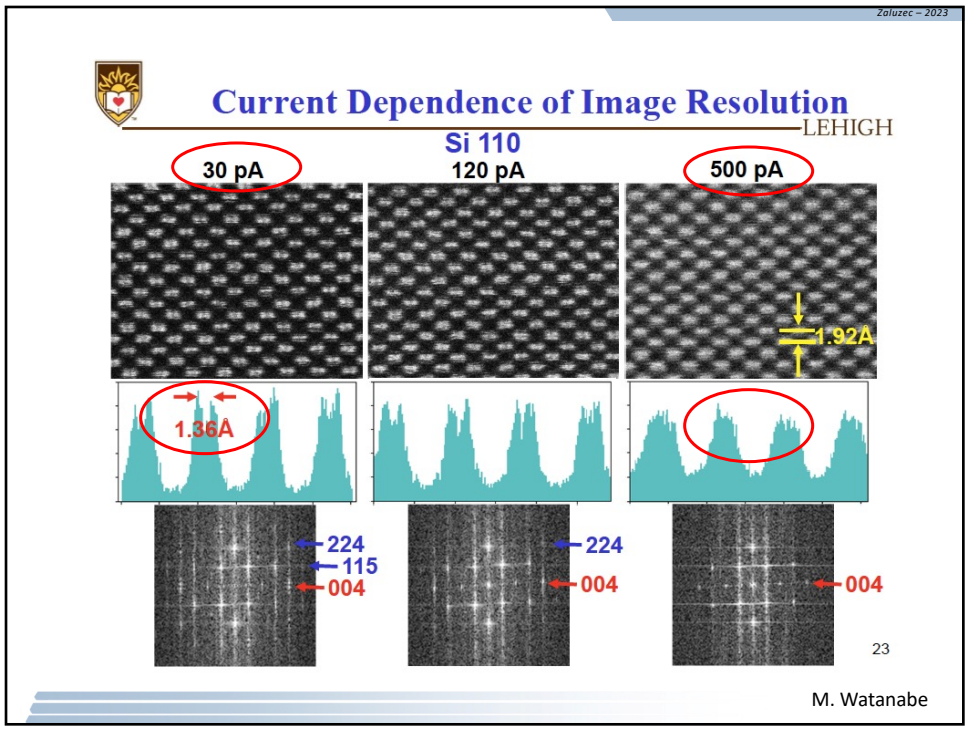
Zaluzec – 2023
Current Dependence of Image Resolution
LEHIGH
Si 110
30 pA
120 pA
500 pA
1.92Å
1.36Å
224
115
004
224
004
004
23
M. Watanabe

46

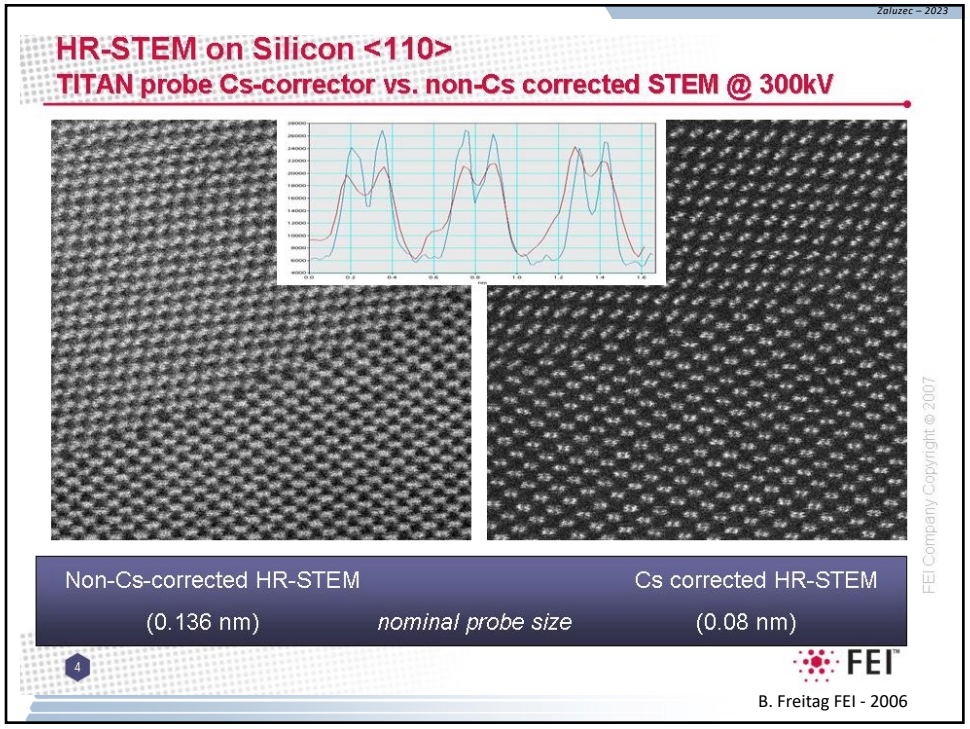
Zaluzec – 2023
HR-STEM on Silicon <110>
TITAN probe Cs-corrector vs. non-Cs corrected STEM @ 300kV
Non-Cs-corrected HR-STEM
(0.136 nm)
nominal probe size
Cs corrected HR-STEM
(0.08 nm)
FEI Company Copyright © 2007
4
FEI
B. Freitag FEI - 2006

47

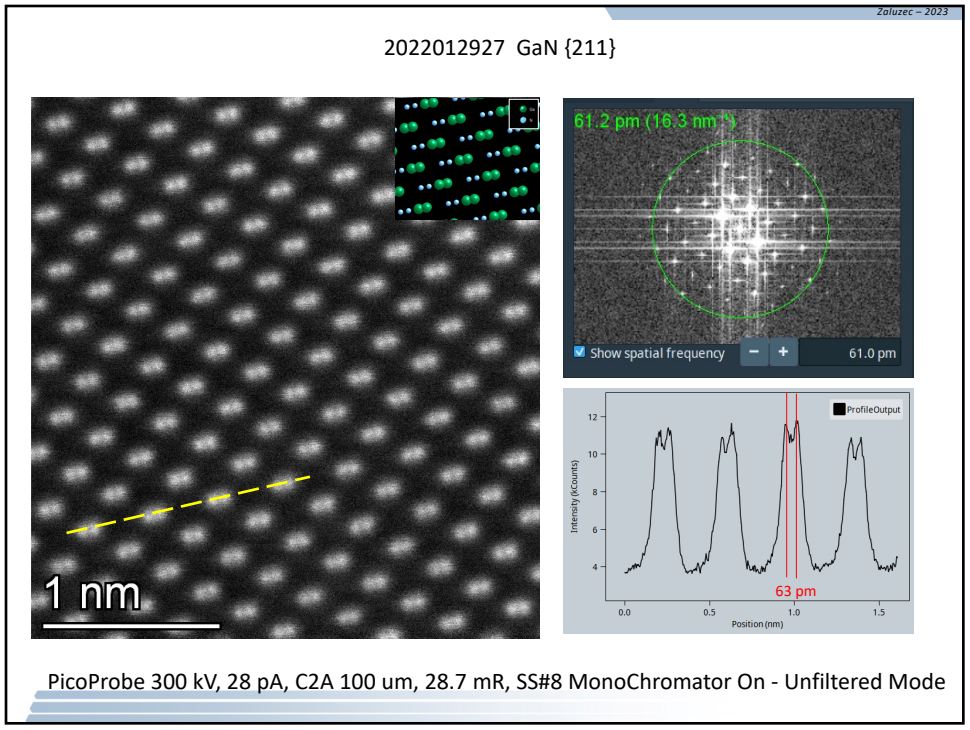
Zaluzec – 2023
2022012927 GaN {211}
1 nm
61.2 pm (16.3 nm⁻¹)
Show spatial frequency
61.0 pm
ProfileOutput
Intensity (kCounts)
Position (nm)
63 pm
PicoProbe 300 kV, 28 pA, C2A 100 um, 28.7 mR, SS#8 MonoChromator On - Unfiltered Mode

48

Zaluzec – 2023

TEAM Project

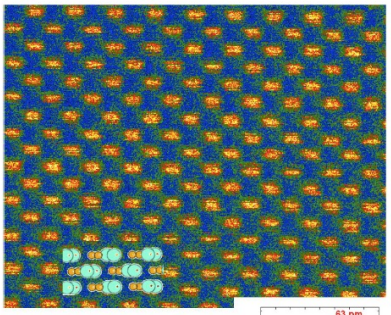

GaN [211]

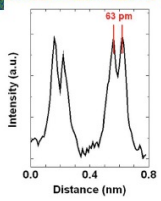

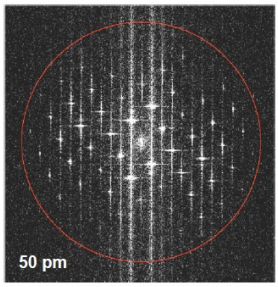

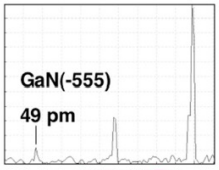

24

49

Zaluzec – 2023

Scanning Confocal Electron Microscopy
Depth Profiling

Aberration-correction allows for larger probe-forming aperture angles.As aperture angle increases, probe width decreases. Moreover "depth of focus"decreases, and even more rapidly.

By varying defocus, in additional to usual 2D raster scan, could now scan in 3D.Can still measure several signals simultaneously.

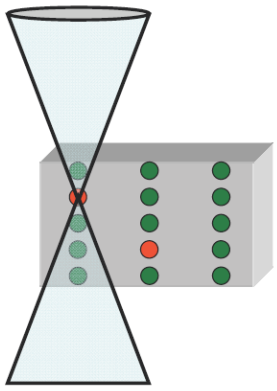

50

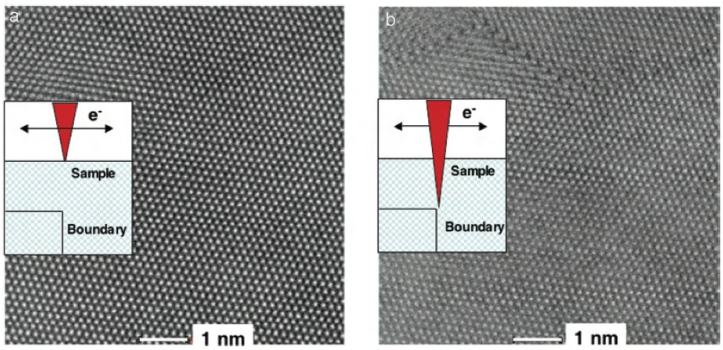

Figure 5. HAADF STEM images of gold [111]: (**a**) STEM probe focused on sample surface as indicated by the schematic; (**b**) Σ3 {112} grain boundary in the lower section of the foil (see inset schematic) is revealed only when the probe is focused 6 nm into the sample.

Microsc. Microanal. 14, 454–462, 2008
doi:10.1017/S1431927608080902

51

Scanning Confocal Optical Microscopy

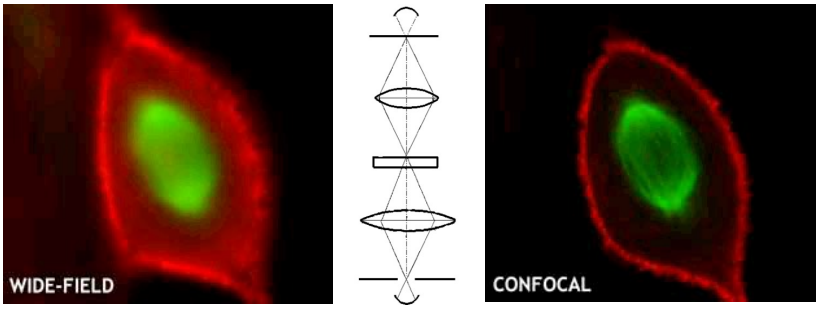

http://www.itg.uiuc.edu/technology/atlas/microscopy/confocal.htm

52

Scanning Confocal Electron Microscopy

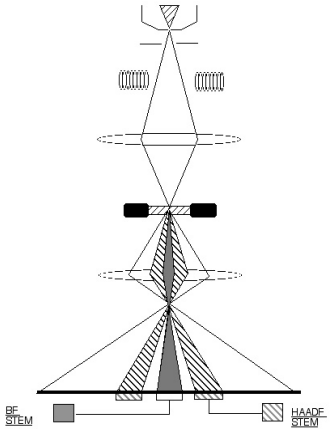

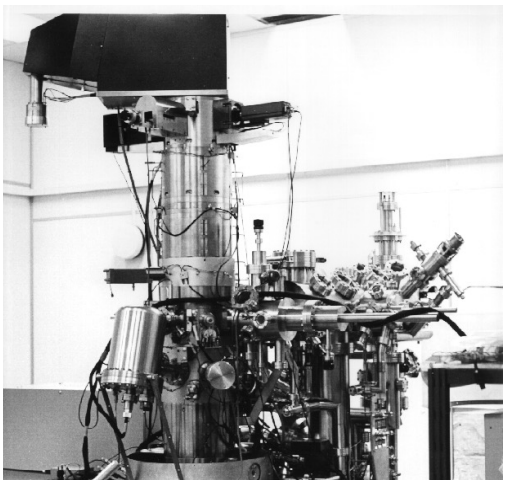

53

Comparison TEM/SCEM
Semiconductor Specimen

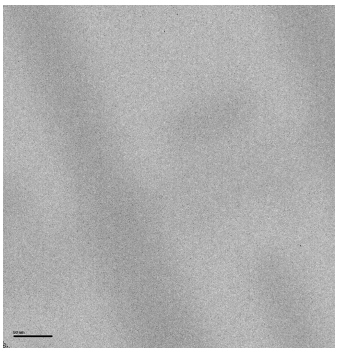

TEM

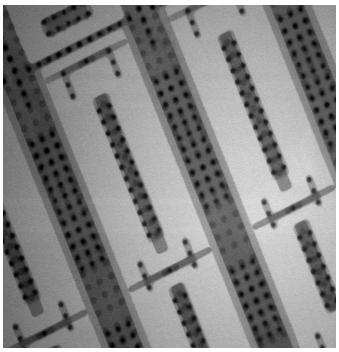

SCEM

" ~ 3+ µmThick"

54

Comparison of TEM/SCEM imaging
5 µm thick X-section of hair medulla

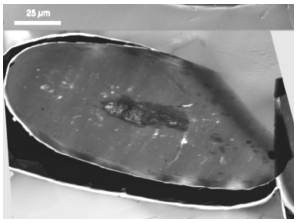

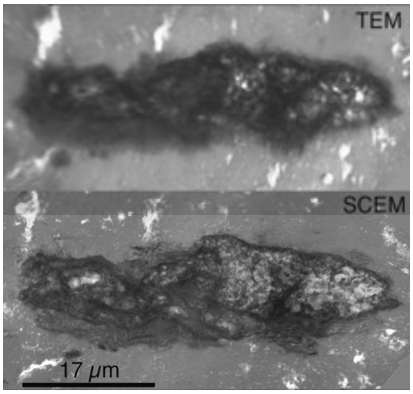

P. Hallegot & N. J. Zaluzec
Scanning Confocal Electron Microscopy of Thick Biological Materials
Microscopy & Microanalysis 2004, Savannah Ga

55

Comparison of TEM/SCEM imaging
5 µm thick X-section of hair medulla

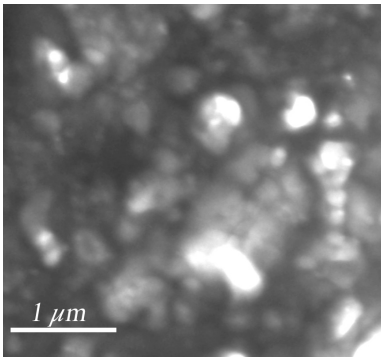

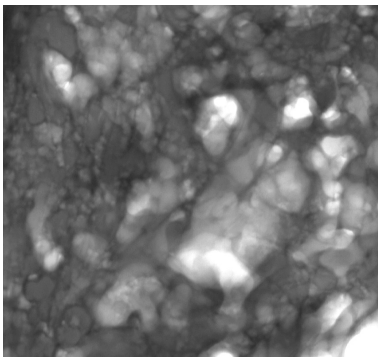

TEM **SCEM**

P. Hallegot & N. J. Zaluzec
Scanning Confocal Electron Microscopy of Thick Biological Materials
Microscopy & Microanalysis 2004, Savannah Ga

56

Depth of Focus/Field
Pre vs Post Specimen Semi-Angles

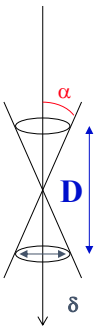

$$D = \frac{\delta}{\alpha}$$

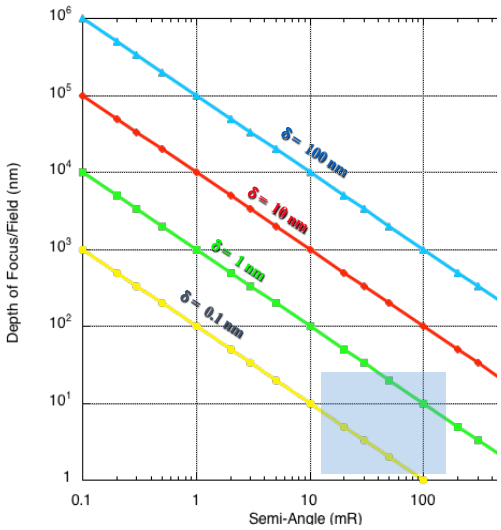

Useful Targets Require Aberration Correctors

57

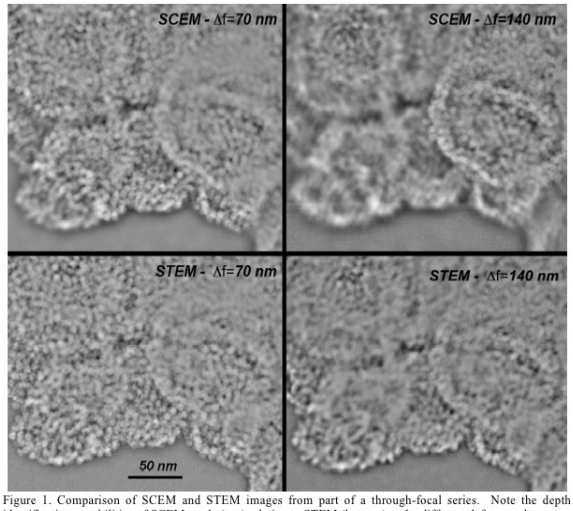

Figure 1. Comparison of SCEM and STEM images from part of a through-focal series. Note the depth identification capabilities of SCEM mode (top) relative to STEM (bottom) at the different defocus values.

Weyland, Etheridge, Zaluzec M&M 2009

58

Zaluzec – 2023

Focal series of a 16-layered silicon <110> with a Ge-substitute at the 8th layer

Accelerating voltage: 50kV, thickness 28.9Å,
C7=4mm, illumination angle: 150 mrad

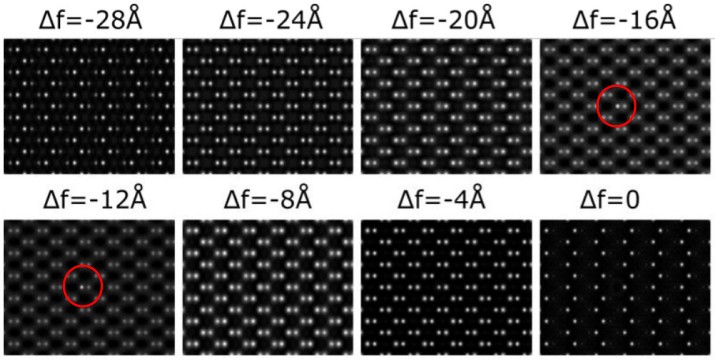

Cs, Cc -> 0

Courtesy of H. Rose
Calculations 2016

59

Zaluzec – 2023

What are the Limits - Today?

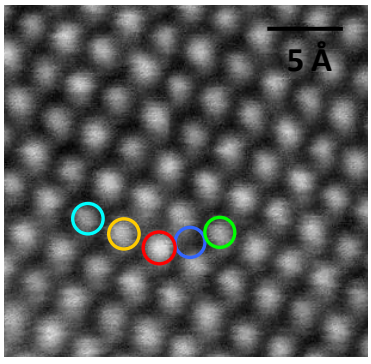

La in $CaTiO_3$ grown by MBE

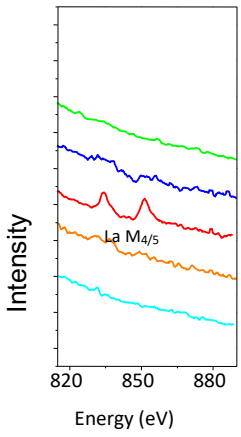

Spectroscopic identification at subnanometer resolution.

8% collection efficiency

S. Pennycook from the TEAM Project Report

60